MULTIPLE CRACKING IN THERMAL FATIGUE

A. Fissolo and B. Marini*

Experiments were carried out on 316L steel. As for true components, thermal cycles have been repeatedly applied on surface of specimen. Main evolutions of the multiple cracking network are analyzed using an image analysis device.

A modelling is proposed to predict growth evolutions in the depth direction. Crack initiation is obtained with a stochastic simulation, growth is estimated with an effective stress intensity factors method. In spite of simplified assumptions, it gives mean values in relatively good agreement with observations.

INTRODUCTION

The multiple cracking problem has received attention in recent years, mainly because it presents a very important issue in the prediction of component life. It can be observed with many different situations, such as stress corrosion cracking, fatigue corrosion fatigue and thermal fatigue. This study deals with multiple cracking development in thermal fatigue. A cracking network was observed on several industrial components, such as moulds used in the fabrication of centrifugally-cast iron tubes (1), expansion tank of fast breeder reactors (2).

To reproduce the in-service cracking, thermal fatigue facilities were built. As for true components, thermal loadings are generated from temperature gradients in the thickness. As previously presented, initiation and propagation of a single crack can be predicted (3). However, tests show clearly that

* CEA - CEREM Service des Recherches Métallurgiques Appliquées, Commissariat à l'Energie atomique - Saclay, 91 191 Gif sur Yvette, France

interaction effects must be taken into account in the case of multiple cracks. So, an objective of the present paper is to obtain an efficient modelling to predict multiple cracks length in the depth direction. In this frame, a specific campaign and methodology has been developed.

EXPERIMENTAL PROCEDURES

The material studied is an AISI 316L stainless steel, its chemical composition is given in Table 1 :

TABLE 1- Chemical composition (wt %) of 316 L steel.

C	Ni	Cr	Mn	Cu	Mo	Si	Co	S	P	N	B	Fe
0.024	12.33	17.44	1.82	0.2	2.3	0.46	0.17	0.001	0.003	0.06	0.0008	Bal.

The average grain size is situated between 3 and 4.(ASTM-E112-74).

The thermal loading cycling is obtained with the SPLASH facility. The specimen is heated by the passage of an electrical current (Figure 1). Two opposite faces are simultaneously cooled by spraying water. Temperature measurements and calculations show that temperature does not change significantly at the core during quenching. Thus, the temperature range on the surface is the same as the temperature range between surface and core. During the test, temperatures are continually controlled using thermocouple measurements (±5°C). Calibration of the thermal loading results from measurements performed with a specific specimen. All the multiple cracking tests were performed for a surface temperature variation between 300 and 550 °C as illustrated on Figure 2.

When tests are ended, surface cracking is first observed with a light microscope. After, to investigate accurately cracking evolutions under the surface, specimens were sectioned and thin surface layers step by step removed.

To obtain morphology characteristics of the cracking network, photographs are digitalized using an image analysis device.

EXPERIMENTAL RESULTS

Cracking path is clearly intragranular. A significant reduction of the grain size is exhibited in the surface zone of about 10 μm. Electron-beam scattering pattern and X-ray diffraction examinations confirm this phenomenon.

Figure 3 presents the morphology of the cracking network after 100,000 cycles. A very strong decrease of the cracking density is observed with the depth. If

many cracks are progressively stopped, others continue to develop. Such behaviour points out a very important shedding effect .But, no any cracking is present beyond 2.1 mm depth. Figure 4 shows the low influence of number of cycles on cracking density after 20,000 cycles. The evolution corresponds mainly to an extension of some longer cracks. Let us note that spacing distance between crack is about 150 – 200 μm at the surface, which corresponds to 1 – 2 grains.

MODELLING

The aim of the modelling is to estimate crack growth evolutions in the depth direction.

Basis of the modelling. As showed by experiments, two separate steps must be distinguished for the multiple cracking evolution : initiation and crack propagation.

The first step corresponds to formation of the cracks. Grains on surface were generated using a Monte-Carlo randomisation method : size distributions are deduced from experimental observations. After, it is assumed that each grain is cracked.

The second step corresponds to extension of the multiple cracks. The methodology is extrapolated from that employed to predict the growth of the single cracks. In that case, it allowed to give good predictions, even when non-negligible plasticity occurs (4). A first step is devoted to the determination of an equivalent stress range $\Delta\sigma_{eq}$, which is perpendicular to the crack plane. It is derived from a fictitious elastic distribution having the same distribution as that obtained from an elastic-plastic analysis. So the equivalent stress range is the sum of two terms. The first is equal to the stress range multiplied by the factor measuring the crack closure phenomenon (stress range for which the crack is open). The second to a hypothetical elastic stress normal to the crack face, which would produce an elastic strain, equal to the actual plastic strain range.

With such a methodology, cracks are submitted to the equivalent stress range :

$$\Delta\sigma_{eq}(x) = \sum_{i=0}^{i=3} A_i x^i$$

An equivalent stress intensity factor range can be deduced using the superposition method (5). That one is given for a crack of length a by :

$$\Delta K_{eq}(a) = \sqrt{\pi a}\left[A_0 F_1 + \frac{2a}{\pi} A_1 F_2 + \frac{a^2}{2} A_2 F_3 + \frac{4a^3}{3\pi} A_3 F_4 \right]$$

For each crack, only the most influent crack is selected to estimate the shielding interaction effect. In fact, for each crack, a serie of SIF values are estimated by considering all the cracks one by one. Finally, the most influent crack corresponds to the one given the smaller SIF value. Thus, the F_1, F_2, F_3, F_4 factors must now introduced as a function of the respective lengths (a, b) and mutual distance (d) concerning the two selected cracks. These ones were previously calculated using the CEA finite elements code CASTEM 2000.

Finally, growth for each crack is deduced using a Paris relation :

$$a_i(N) = a_{i\,0} + \int_{N_0}^{N} C\Delta K_{eq}[i]^m dn \qquad \text{with C} = 2.05\ 10^{-10} \text{ and m} = 4.2$$

Note that the Paris relation, used for estimations, corresponds to the mean fatigue crack growth obtained on a very important 316LN data base (6).

Initial lengths a_{io} obtained after applying of N_0 thermal fatigue cycles, are determined with a random Monte-Carlo simulation. Crack length is simply calculated step by step after a progressive revaluation of the term ΔK_{eff}. Revaluations are performed only with the most influent crack. For a given crack, that one is not necessarily the same during all the growing phase.

Results of the simulation.

Figure 5 presents different phases of the cracks extension in the depth direction for a same random initiation. Maximum depth reaches about of 3.5 mm after 100,000 cycles. As observed on experiments, a very strong shielding effect is obtained. Furthermore, the experimental relation between depth and spacing is reproduced (Figure 6).

In order to estimate influence of the random initiation on the growing phase, 10 different simulations have been successively computed (Figure 7). A very weak influence of initial distribution is evidenced concerning the mean depth. Let us note that simulated values are not very far from measurements. For maximum depth, scattering becomes more important and values are overestimated.

CONCLUSION

After an initiation phase, a major part of evolution corresponds to an extension of the longer cracks. A very important shielding effect is evidenced as it was waited for parallels cracks.

In spite of simplifying assumptions, the proposed modelling gives mean values in relatively good agreement with observations. Overestimate of the

maximum depth is probably due to an insufficient evaluation of the shielding effect.

REFERENCES

(1) H. Burlet, S. Vasseur, J. Besson and A. Pineau
Fatigue Engineering Materials 12 – 2, p. 123, 1989.
(2) P. Lemoine, B. Marini, L. Meny
Fatigue à haute température p. 331, Journée Internationale de Printemps, 1986.
(3) A. Fissolo, B. Marini, G. Nais, P. Wident
Journal of Nuclear Materials 233 – 237, p. 156 – 161, 1996.
(4) J.R. Haigh and R.P. Skelton
Materials Science Engineering, 36, p. 133, 1978.
(5) C.B. Buchalet and W.H. Bamford
Mechanics of Crack Growth, ASTM STP 590, p. 385 – 402, 1976.
(6) A.A. Tavassoli
Fusion Engineering and Design 29, p. 371 – 390, 1995.

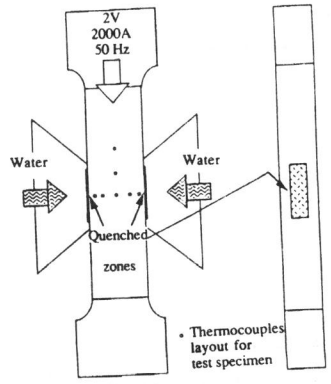

Figure 1 : Thermal fatigue test facility Splash

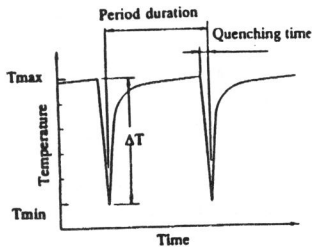

Figure 2 : Temperature variation at the surface

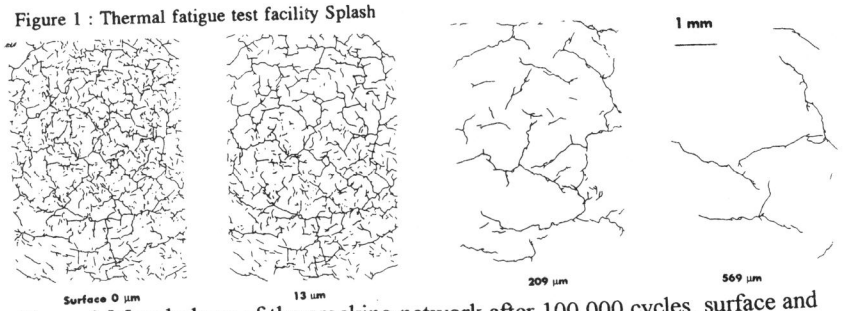

Figure 3 Morphology of the cracking network after 100,000 cycles. surface and after thin surface layers step by step removed.

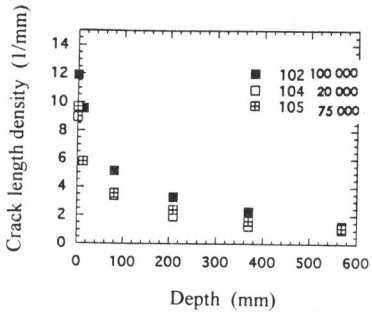

Figure 4 Cracking length density as a function of depth. Examinations performed after thin surface layers step by step removed.

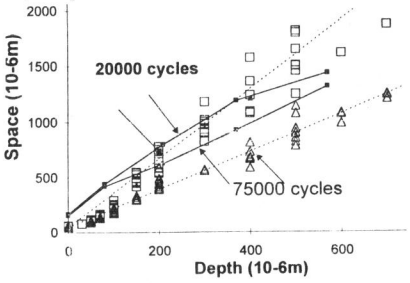

Figure 6 Simulation (dotted lines) and experimental data - Relation between spacing and depth at 20 000 and 75000 cycles.

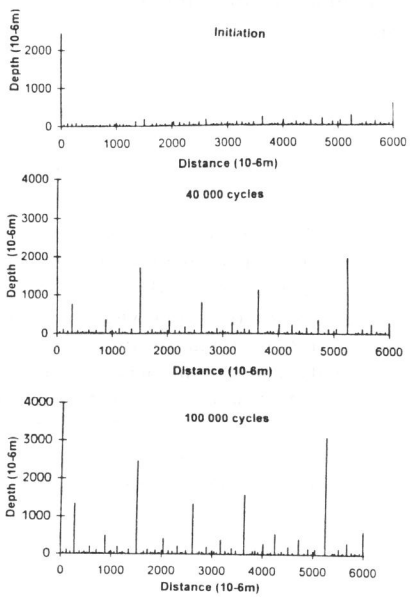

Figure 5 Simulation - Different phases of the cracks extension in the depth direction.

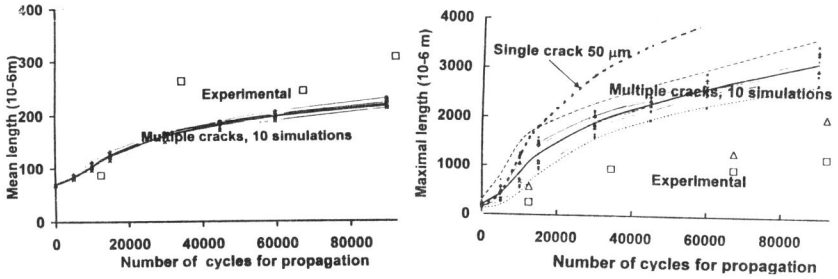

Figure 7 Simulation and experimental data – maximum and mean crack depth as a function of numbre of cycles for propagation.
For simulation, 10 series of cracks were successively generated.